Reducing Time Headway for Platooning of Connected Vehicles via V2V Communication

Yougang Bian[a], Yang Zheng[a,b], Wei Ren[c], Shengbo Eben Li[a,*], Jianqiang Wang[a,d], Keqiang Li[a,*]

[a]*State Key Laboratory of Automotive Safety & Energy, Department of Automotive Engineering, Tsinghua University, Beijing, China*
[b]*Department of Engineering Science, University of Oxford, Oxford, UK.*
[c]*Department of Electrical and Computer Engineering, University of California, Riverside, Riverside, USA.*
[d]*Collaborative Innovation Center of Electric Vehicles in Beijing, Beijing, China*

Abstract

In a platoon of connected vehicles, time headway plays an important role in both traffic capacity and road safety. It is desirable to maintain a lower time headway while satisfying string stability in a platoon, since this leads to a higher traffic capacity and guarantees the disturbance attenuation ability. In this paper, we study a multiple-predecessor following strategy to reduce time headway via vehicle-to-vehicle (V2V) communication. We first introduce a new definition of desired inter-vehicle distances based on the constant time headway (CTH) policy, which is suitable for general communication topologies. By exploiting lower-triangular structures in a time headway matrix and an information topology matrix, we derive a set of necessary and sufficient conditions on feedback gains for internal asymptotic stability. Further, by analyzing the stable region of feedback gains, a necessary and sufficient condition on time headway is also obtained for the string stability specification. It is proved that a platoon can be asymptotically stable and string stable when the time headway is lower bounded. Moreover, this bound can be reduced by increasing the number of predecessors. These results explicitly highlight the benefits of V2V communication on reducing time headway for platooning of connected vehicles.

Keywords: Connected vehicles, constant time headway, multiple-predecessor following, V2V communication, string stability

1. Introduction

The increase of car ownership has posed a high demand on road throughput as well as transport safety and efficiency. To mitigate this issue, one promising approach is the cooperation of multiple connected vehicles using onboard sensors and vehicle-to-vehicle (V2V) communication. As discussed in (Talebpour & Mahmassani, 2016; Xu et al., 2018; Lioris et al., 2017), the cooperation of connected vehicles has the potential to greatly improve throughput and safety for both urban and highway traffic. In the one-dimensional case, this cooperation technique is referred to as the cooperative adaptive cruise control (CACC) or vehicular platooning (Shladover, 2007; Shladover et al., 1991). A review of recent advances in platoon control can be found in (Li et al., 2017b).

In a vehicular platoon, multiple connected vehicles are coordinated to move in a one-dimensional formation. In this formation, the most important properties include the internal stability and string stability. The internal stability indicates the ability to maintain the formation asymptotically, which requires that all eigenvalues of the system characteristics polynomial are in the open left half plane. Different from this, the string stability represents the ability to attenuate the effects of disturbances along the platoon (Seiler et al., 2004). In the literature, there are different types of definitions for string stability, such as the L_2 (Ploeg et al., 2014a; Al-Jhayyish & Schmidt, 2018), L_p (Ploeg et al., 2014b), L_∞ (Stüdli et al., 2017), and head-to-tail string stability (Ge & Orosz, 2014, 2018; Wang, 2018). It is known that the string stability is highly influenced by the range policy, *i.e.*, how the desired inter-vehicle distances are defined. Commonly used range policies include: 1) the constant spacing (CS) policy, and 2) the

*Corresponding author
Email addresses: byg14@mails.tsinghua.edu.cn (Yougang Bian), yang.zheng@eng.ox.ac.uk (Yang Zheng), ren@ece.ucr.edu (Wei Ren), lishbo@tsinghua.edu.cn (Shengbo Eben Li), wjqlws@tsinghua.edu.cn (Jianqiang Wang), likq@tsinghua.edu.cn (Keqiang Li)

constant time headway (CTH) policy. In the CS policy, the desired inter-vehicle distance is a constant value, which has the best potential to reduce the platoon length and thus improve road throughput. In the case of the CS policy, string stability cannot be achieved using identical linear feedback controllers for the predecessor-following (PF) topology (Seiler et al., 2004; Darbha & Hedrick, 1999; Naus et al., 2010) and bi-directional (BD) topology (Barooah & Hespanha, 2005). One solution is to broadcast the leader's information, yielding the predecessor-leader following (PLF) topology (Darbha & Hedrick, 1999). This strategy poses a high requirement on communication channels as the platoon length grows. Another method is to use asymmetric controllers (Khatir & Davison, 2004; Ghasemi et al., 2013), which may cause the feedback gains to increase with the platoon size. A more recent discussion on the CS policy can be found in (Konduri et al., 2017). In the CTH policy, the desired inter-vehicle distance has a linear relationship with the velocity, which agrees with human drivers' characteristics to some extent. In the case of the CTH policy, string stability can be achieved without the dependence on the leader's information (Ploeg et al., 2014a; Naus et al., 2010). In particular, to guarantee string stability, the requirement on time headway has a strong connection with the time lag and delay in the vehicle control loop. For example, in (Darbha & Rajagopal, 2001), it is proved that the time headway must be two times larger than the time lags in the actuation and sensing systems. This result has been further extended to account for the parasitic time delays (Xiao & Gao, 2011). In some studies, the leaders' information is also used for platoons with the CTH policy, *e.g.*, (Milanés et al., 2014a,b; Chehardoli & Ghasemi, 2018). Introducing time headway may compromise the transport throughput, since the inter-vehicle distance increases as the velocity grows. It is therefore desirable to reduce time headway while guaranteeing string stability (Flores & Milanés, 2018).

In addition to the commonly used CS and CTH policies mentioned above, other types of nonlinear range policies were also studied. For example, a quadratic range policy based on human driving data was proposed in (Zhou & Peng, 2005) to improve traffic flow stability and string stability; an adaptive range policy for platoons with the PLF topology was proposed in (Rödönyi, 2018) to address the unknown predecessor range policy; a delay-based range policy was proposed in (Besselink & Johansson, 2017) to guarantee string stability when disturbances exist. Besides, different control methods were studied to meet the specification of string stability, such as model predictive control (Dunbar & Caveney, 2012), H_∞ control (Ploeg et al., 2014a), sliding mode control (Xiao & Gao, 2011; Kwon & Chwa, 2014; Guo et al., 2016), adaptive control (Kwon & Chwa, 2014; Guo et al., 2016; Chehardoli & Ghasemi, 2018), and fractional-order PD control (Flores & Milanés, 2018). We note that these methods typically rely on the CTH policy or require certain leader's information for local feedback when using the CS policy.

Recently, the rapid development of V2V techniques enriches the types of information flow topologies, which brings benefits as well as challenges to the analysis and design of platoon systems. With the introduction of V2V communication, a platoon system can be more appropriately viewed as a multi-agent system (Jadbabaie et al., 2003; Ren & Beard, 2008; Olfati-Saber et al., 2007; Ren & Cao, 2010), for which graph theory can be applied to systematically address the modeling and synthesis problems (Yadlapalli et al., 2006; Zheng et al., 2016; Petrillo et al., 2018; Li et al., 2017a). For example, Fax & Murray (2004) introduced a separation principle to reduce the formation stability into the information flow stability and the individual vehicle stability. Yadlapalli et al. (2006) showed a tradeoff between communication and scalable controllers, and proved that at least one vehicle should maintain a large number of communication links in a rigid platoon to guarantee the existence of scalable controllers. Zheng et al. (2016) proposed a four-component framework to systematically study the influence of information flow topologies on vehicular platoons in terms of the internal stability, scalability, and robustness; see, also, Zheng et al. (2018). Similar methods have been used in (Petrillo et al., 2018; Li et al., 2017a) by exploiting the decomposability of information topology matrices. These studies provide certain insights on the influence of V2V communication on platoons with the CS policy. However, string stability may still be unsatisfied for platoons with the CS policy (Konduri et al., 2017). Therefore, it remains to be an important topic to address the effect of information flow topologies on platoons with the CTH policy.

We note that a few recent studies have offered some progress (Chehardoli & Homaeinezhad, 2017; Darbha et al., 2017, 2018). In these studies, the definitions of the CTH policy are inconsistent with each other. In principal, time headway denotes the time that it takes for the host vehicle to cover the distance between its own and its predecessor's front bumpers. For a platoon with the PF topology, the desired inter-vehicle distance directly depends on the host vehicle's velocity. As for general information flow topologies, such as the multiple-predecessor following (MPF) and the multiple-predecessor-leader following (MPLF) topologies, the definition of desired inter-vehicle distances may have different choices. For example, in (Chehardoli & Homaeinezhad, 2017), the leading vehicle's velocity is used to define desired inter-vehicle distances for platoons with the MPLF topology, while in (Darbha et al., 2017, 2018), the host vehicle's velocity is used for platoons with the MPF topology. These definitions either rely on the leading

vehicle's information or may cause inconsistency in desired inter-vehicle distances (see Section 3 for details).

In this paper, we study the effects of V2V communication on platoons with the CTH policy. Specifically, we aim to exploit the MPF strategy to reduce time headway and improve road throughput. First, we introduce a new definition of inter-vehicle distances using CTH, which avoids inconsistency in desired inter-vehicle distances. Then, we investigate how to reduce the time headway for platoons with the MPF topology via V2V communication. Based on the results on the internal stability and string stability, we show that increasing the number of predecessors can reduce the bound of allowable time headway. Precisely, our main contributions are:

1. A new definition of desired inter-vehicle distances using CTH is introduced for general information flow topologies under V2V communication. This definition is a straightforward extension of that in the PF topology, and can avoid inconsistency in desired inter-vehicle distances.
2. A set of necessary and sufficient conditions on feedback gains is derived for internal asymptotic stability, which depicts a stability region for feedback gains and gives a lower bound of allowable time headway for internal asymptotic stability. Our result extends that in (Zheng et al., 2016, 2019) from platoons with the CS policy to platoons with the CTH policy.
3. Further, another set of necessary and sufficient conditions on feedback gains is derived for the string stability specification. This condition gives another lower bound of allowable time headway for string stability. We show that increasing the number of predecessors allows one to reduce the bound of allowable time headway. This phenomenon is consistent with the results in (Darbha et al., 2017, 2018), where a different spacing policy was used. Compared with the previous works, one highlight of our results is that the analytical feasible region of feedback gains is derived in terms of both internal asymptotic stability and string stability, which explicitly shows the effects of V2V communication on platoon systems. Some preliminary results was summarized in (Bian et al., 2018).

The rest of this paper is organized as follows. Section 2 presents the system modeling, and Section 3 gives the definition of the desired inter-vehicle distances using CTH. We present the results on internal stability and string stability in Section 4 and 5, respectively. Numerical experiments are given in Section 6, and we conclude the paper in Section 7.

Notations: The fields of integers, real numbers, and $m \times n$ real matrices are denoted by $\mathbb{Z}$, $\mathbb{R}$, and $\mathbb{R}^{m\times n}$, respectively. A matrix $M \in \mathbb{R}^{m\times n}$ is represented by its entries m_{ij}, $i \in \{1, 2, \dots, m\}$, $j \in \{1, 2, \dots, n\}$, *i.e.*, $M = [m_{ij}]$, and its transpose and conjugate transpose are denoted by $M^\top$ and M^{H}, respectively. A diagonal matrix $M \in \mathbb{R}^{n\times n}$ with diagonal entries $m_1, m_2, \dots, m_n$ is denoted by $\mathrm{diag}\{m_1, m_2, \dots, m_n\}$. The $n \times n$ identity matrix is denoted by I_n. For any positive integer N, the set of $\{1, 2, \dots, N\}$ is denoted by $\mathcal{N}$. The intersection and union of two sets A and B are denoted by $A \cap B$ and $A \cup B$, respectively. The AND-operation and OR-operation of two propositions A and B are denoted by $A \wedge B$ and $A \vee B$, respectively. Finally, the symbol "$\Longrightarrow$" means "if $\cdots$, then $\cdots$", and "$\Longleftrightarrow$" denotes "if and only if $\cdots$".

2. System modeling

We consider a platoon of connected vehicles that consists of 1 leader and N followers, indexed by 0 and $1, 2, \dots, N$, respectively. The road is assumed to be straight and flat so the lateral vehicle motion is neglected for convenience. The control objective is to coordinate the longitudinal motion of connected vehicles so that they keep the desired inter-vehicle distance while maintaining the desired velocity. As suggested in (Zheng et al., 2016), we model a platoon system from four aspects: (1) vehicle dynamics, which describe the longitudinal behavior of each vehicle; (2) information flow topology, which defines how vehicles exchange information with each other; (3) formation geometry, which depicts the desired inter-vehicle distances; (4) distributed controller, which implements feedback control law on each vehicle based on local information.

2.1. Vehicle dynamics

In this paper, we use a linear third-order model to represent the dynamics of the leading and following vehicles:

$$\begin{cases} \dot{p}_i = v_i, \\ \dot{v}_i = a_i, \\ \tau_i \dot{a}_i + a_i = u_i, \end{cases} \qquad i \in \{0\} \cup \mathcal{N}, \tag{1}$$

where p_i, v_i, and a_i denote the position, velocity and acceleration, respectively; $\tau_i > 0$ is the inertial time lag in the powertrain. In model (1), it is assumed that each vehicle is equipped with a low-level acceleration controller that regulates a_i according to u_i. The powertrain system is approximated as a first-order inertial system with a heterogeneous time constant τ_i. This model is simple yet accurate enough for platoon level synthesis, which is widely used in the literature, *e.g.*, (Zhou & Peng, 2005; Zheng et al., 2016; Darbha et al., 2017). We note that nonlinear vehicle dynamics are also used in (Dunbar & Caveney, 2012; Kwon & Chwa, 2014; Zheng et al., 2018). However, in that case, explicit results are rather difficult to derive. A comparison of different models was discussed in (Li et al., 2015).

2.2. Information flow topology

In this study, we assume that there is no communication delay or packet loss. Typical studies on platoons subject to communication delays and packet losses can be found in (di Bernardo et al., 2015; Zhang & Orosz, 2016; Petrillo et al., 2018; Harfouch et al., 2018). The information flow topology among the following vehicles is modeled with a directed graph $\mathcal{G}(\mathcal{V}, \mathcal{E}, \mathcal{A})$, where $\mathcal{V} = \{v_1, v_2, \ldots, v_N\}$ is a set of nodes representing all the following vehicles, $\mathcal{E} \subseteq \mathcal{V} \times \mathcal{V}$ is a set of edges representing the connections between each pair of following vehicles, and $\mathcal{A} = [a_{ij}] \in \mathbb{R}^{N\times N}$ is an adjacency matrix, defined as

$$a_{ij} = \begin{cases} 1, & \text{if } \{v_j, v_i\} \in \mathcal{E}, \\ 0, & \text{otherwise}, \end{cases} \quad i, j \in \mathcal{N}, \tag{2}$$

where $\{v_j, v_i\} \in \mathcal{E}$ means that vehicle i can acquire the information of vehicle j. Besides, it is assumed that there is no self-loop, *i.e.*, $a_{ii} = 0, \forall i \in \mathcal{N}$. The property of $\mathcal{G}$ is further characterized with the following two matrices.

1. The degree matrix associated with $\mathcal{G}$ is defined as $\mathcal{D} = \text{diag}\{d_{11}, d_{22}, \ldots, d_{NN}\} \in \mathbb{R}^{N\times N}$ with

$$d_{ii} = \sum_{k=1}^{N} a_{ik}, \quad i \in \mathcal{N}. \tag{3}$$

   Essentially, d_{ii} describes the number of following vehicles of which the information is available for vehicle i.
2. The Laplacian matrix associated with $\mathcal{G}$ is defined as $L = [l_{ij}] \in \mathbb{R}^{N\times N}$ with

$$l_{ij} = \begin{cases} -a_{ij} & i \neq j, \\ \sum_{k=1}^{N} a_{ik} & i = j, \end{cases} \quad i, j \in \mathcal{N}.$$

   According to (2) and (3), it is not difficult to see that $\mathcal{L} = \mathcal{D} - \mathcal{A}$.

To model the connections between the leading vehicle and the following vehicles, we define a pinning matrix:

$$\mathcal{P} = \text{diag}\{p_{11}, p_{22}, \ldots, p_{NN}\} \in \mathbb{R}^{N\times N},$$

where $p_{ii} = 1$ if vehicle i can acquire the information of the leader, and $p_{ii} = 0$ otherwise.

In this study, we consider the MPF topology, *i.e.*, each vehicle can obtain the information of multiple immediate predecessors via V2V communication. Figure 1 gives several examples of the MPF topology. We note that the MPF topology is a direct generalization of the PF and two-predecessor following (TPF) topologies, which are studied in (Ploeg et al., 2014a,b). Here we make the following assumption.

Assumption 1. The connected vehicles in the platoon are interconnected with an MPF topology, and the number of predecessors that vehicle i follows is $r_i \in \mathbb{Z}$, $1 \leq r_i \leq i$, $\forall i \in \mathcal{N}$.

Under Assumption 1, we know $a_{ij} = 0$, $\forall j > i$. Then the adjacency matrix $\mathcal{A}$ becomes a lower-triangular matrix. In addition, we define the following information topology matrix:

$$\mathcal{L}_{\mathcal{P}} := \mathcal{L} + \mathcal{P} = \mathcal{D} - \mathcal{A} + \mathcal{P}.$$

Also, it is easy to see that $\mathcal{L}_{\mathcal{P}}$ is a lower-triangular matrix, since both $\mathcal{D}$ and $\mathcal{P}$ are diagonal matrices. Moreover, the diagonal elements of $\mathcal{L}_{\mathcal{P}}$ are $d_{ii} + p_{ii} = r_i$.

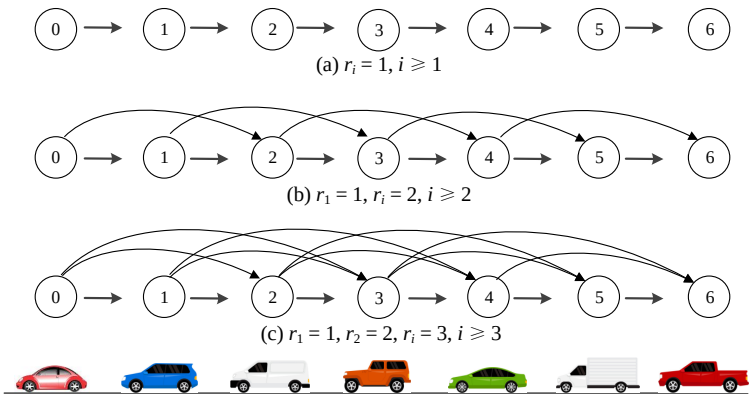

Figure 1: Examples of the MPF topology (r_i is the number of predecessors of vehicle i)

2.3. Formation geometry

The desired formation geometry of the platoon is defined with desired inter-vehicle distances. In detail, the desired distance between vehicle i and the leader 0 is $d_{i,0}(t)$, of which the precise definition will be given in (8). Then, the control objective is formulated as

$$\begin{cases} \lim\limits_{t\to+\infty} \big\|p_i(t) - p_0(t) + d_{i,0}(t)\big\| = 0, \\ \lim\limits_{t\to+\infty} \big\|v_i(t) - v_0(t)\big\| = 0, \\ \lim\limits_{t\to+\infty} \big\|a_i(t) - a_0(t)\big\| = 0, \end{cases} \qquad \forall i \in \mathcal{N}. \tag{4}$$

This objective takes the leader's information as a reference trajectory, which is a global coordination. However, the leader may not be connected to all the followers in practice. Indeed, this objective should be achieved using local information in a distributed way; see the next subsection.

2.4. Distributed controller

We consider the following linear feedback controller:

$$u_i = -\sum_{j=1}^{N} a_{ij}\big(k_{ip}(\tilde{p}_i - \tilde{p}_j) + k_{iv}(\tilde{v}_i - \tilde{v}_j) + k_{ia}(\tilde{a}_i - \tilde{a}_j)\big) - p_{ii}(k_{ip}\tilde{p}_i + k_{iv}\tilde{v}_i + k_{ia}\tilde{a}_i), \tag{5}$$

where k_{ip}, k_{iv}, and k_{ia} are the feedback gains; $\tilde{p}_i$, $\tilde{v}_i$, and $\tilde{a}_i$ are the position, velocity, and acceleration tracking errors with respect to the leading vehicle, respectively, and their precise definitions are given in (9). Note that in this controller, only local information, *i.e.*, the neighbors' information, is used for feedback, since $\tilde{p}_i - \tilde{p}_j$ denotes the relative position error between vehicle i and vehicle j; see (9). In essence, we aim to use local information to design feedback input (5) for each follower, such that the global coordination (4) is achieved in a platoon level. Note that p_{ii} can be either 1 or 0 depending on whether follower i can communicate with the leader (not all the vehicles can obtain the leader's information).

3. Desired inter-vehicle distances using CTH

In this section, we introduce the desired inter-vehicle distances using CTH. For the CTH policy in the PF topology, the desired inter-vehicle distance between vehicle i and $i-1$ is naturally defined as

$$d_{i,i-1} = h_i v_i + D, \tag{6}$$

where h_i is the time headway, and D is the standstill gap. When it comes to general information flow topologies, the definitions of desired inter-vehicle distances are not consistent in the literature. For example, in (Chehardoli

& Homaeinezhad, 2017), the desired distance between vehicle i and $i-l$ is defined as $d_{i,i-l} = \sum_{k=i-l}^{i-1} h_k v_0 + lD$, where v_0 is the leading vehicle's velocity, and h_k is the time headway of vehicle $k-1$ with respect to vehicle k. This definition is based on the leading vehicle's velocity, implying that each vehicle must obtain the leader's information. In (Darbha et al., 2017, 2018), the desired inter-vehicle distance between vehicle i and $i-l$ is defined as $d_{i,i-l} = lhv_i + lD$, where h is the time headway of vehicle i with respect to vehicle $i-l$. This definition is based on the velocity of the host vehicle only. However, this leads to inconsistency in desired inter-vehicle distances in the transient process, *i.e.*, $d_{i,k}(t) \neq d_{i,j}(t) + d_{j,k}(t)$ if $v_i(t) \neq v_j(t)$. Similar issues are also considered in (Rödönyi, 2018) when the predecessor's range policy is unknown.

In this study, we directly extend the definition of the CTH policy of the PF topology to general topologies, by adding the desired inter-vehicle distances, given in (6), *i.e.*,

$$d_{i,i-l} = \sum_{k=i}^{i-l+1} (h_k v_k + d_k), \tag{7}$$

where $h_k \geq 0$ and $d_k > 0$ are the time headway and desired standstill gap of vehicle k with respect to vehicle $k-1$, respectively. This definition is more intuitive and can avoid inconsistency in desired inter-vehicle distances. It is not difficult to check that:

$$d_{i,k}(t) = d_{i,j}(t) + d_{j,k}(t), \forall t \geq t_0.$$

Note that the new definition (7) relies on the velocities of $l-1$ immediate predecessors, which makes system analysis and controller synthesis nontrivial.

Based on (7), the desired inter-vehicle distance between vehicle i and vehicle 0 becomes:

$$d_{i,0} = \sum_{k=1}^{i} (h_k v_k + d_k). \tag{8}$$

Then the tracking error is defined as:

$$\begin{cases} \tilde{p}_i = p_i + \sum\limits_{k=1}^{i} (h_k v_k + d_k) - p_0, \\ \tilde{v}_i = v_i - v_0, \\ \tilde{a}_i = a_i - a_0, \end{cases} \qquad i \in \mathcal{N}. \tag{9}$$

Note that $\tilde{p}_i$, $\tilde{v}_i$, and $\tilde{a}_i$ in (9) are defined with the information of the leading vehicle for notional simplicity only. Indeed, the calculation of $\tilde{p}_i - \tilde{p}_j$, $\tilde{v}_i - \tilde{v}_j$, and $\tilde{a}_i - \tilde{a}_j$ in the local controller (5) only requires the local information of its predecessors. For example, assume $i > j$, then we have

$$\tilde{p}_i - \tilde{p}_j = p_i - p_j + \sum_{k=j+1}^{i} (h_k v_k + d_k),$$

where vehicle i only uses the information of vehicles j, $j+1$, ..., i.

4. Internal stability analysis

In this section, we first formulate the closed-loop dynamics and then present the internal stability criterion for the closed-loop system. In principle, it is desired that the vehicular platoon runs at a constant velocity. Typically, the variation of the leading vehicle's velocity is viewed as a disturbance on the platoon, which results in a certain transient process. The property of this transient process is studied by using the notion of string stability; see the next section. Here, we make the standard assumption for internal stability analysis (Dunbar & Caveney, 2012; Zheng et al., 2016, 2018) by assuming that the leading vehicle travels in uniform motion. We refer interested readers to the methods in (Cao & Ren, 2012; Baldi & Frasca, 2018), which have the potential to deal with the case of a dynamic leader. Note that these methods generally rely on nonlinear control design, which will pose challenges to string stability analysis.

Assumption 2. The leading vehicle is running at a constant velocity, *i.e.*, $u_0(t) = 0$ and $a_0(t) = 0$.

4.1. Closed-loop dynamics formulation

According to (9) and Assumption 2, we have

$$\begin{cases} \dot{\tilde{p}}_i = \tilde{v}_i + \sum_{k=1}^{i} h_k a_k = \tilde{v}_i + \sum_{k=1}^{i} h_k \tilde{a}_k, \\ \dot{\tilde{v}}_i = \tilde{a}_i, \\ \dot{\tilde{a}}_i = -\frac{1}{\tau_i}\tilde{a}_i + \frac{1}{\tau_i}u_i. \end{cases}$$

Upon denoting the lumped states as $\tilde{p} = [\tilde{p}_1, \tilde{p}_2, \ldots, \tilde{p}_N]^\top$, $\tilde{v} = [\tilde{v}_1, \tilde{v}_2, \ldots, \tilde{v}_N]^\top$, and $\tilde{a} = [\tilde{a}_1, \tilde{a}_2, \ldots, \tilde{a}_N]^\top$, (5) can be rewritten into a compact form as

$$u = [u_1, u_2, \ldots, u_N]^\top = -K_p \mathcal{L}_{\mathcal{P}} \tilde{p} - K_v \mathcal{L}_{\mathcal{P}} \tilde{v} - K_a \mathcal{L}_{\mathcal{P}} \tilde{a}, \tag{10}$$

where $K_\sharp = \mathrm{diag}\{k_{1\sharp}, k_{2\sharp}, \ldots, k_{N\sharp}\}, \sharp \in \{p, v, a\}$. Then we have

$$\begin{cases} \dot{\tilde{p}} = \tilde{v} + H\tilde{a}, \\ \dot{\tilde{v}} = \tilde{a}, \\ \dot{\tilde{a}} = -\Delta K_p \mathcal{L}_{\mathcal{P}} \tilde{p} - \Delta K_v \mathcal{L}_{\mathcal{P}} \tilde{v} - (\Delta + \Delta K_a \mathcal{L}_{\mathcal{P}})\tilde{a}, \end{cases}$$

where H is called the time headway matrix:

$$H := \begin{bmatrix} h_1 & 0 & 0 & 0 \\ h_1 & h_2 & 0 & 0 \\ \vdots & \vdots & \ddots & 0 \\ h_1 & h_2 & \cdots & h_N \end{bmatrix},$$

and Δ is the time lag matrix:

$$\Delta := \begin{bmatrix} \frac{1}{\tau_1} & 0 & 0 \\ 0 & \ddots & 0 \\ 0 & 0 & \frac{1}{\tau_N} \end{bmatrix}.$$

Then the closed-loop dynamics can be described as

$$\dot{\tilde{x}} = \tilde{A}\tilde{x}, \tag{11}$$

where $\tilde{x} = [\tilde{p}^\top, \tilde{v}^\top, \tilde{a}^\top]^\top$ and

$$\tilde{A} = \begin{bmatrix} 0 & I_N & H \\ 0 & 0 & I_N \\ -\Delta K_p \mathcal{L}_{\mathcal{P}} & -\Delta K_v \mathcal{L}_{\mathcal{P}} & -\Delta - \Delta K_a \mathcal{L}_{\mathcal{P}} \end{bmatrix}.$$

In (11), the heterogenous vehicle dynamics are represented by Δ and the structure of $\tilde{A}$; the information flow topology is characterized by $\mathcal{L}_{\mathcal{P}}$; the formation geometry is described by H; and the distributed controller is represented by matrices K_p, K_v, and K_a. This is consistent with the modeling of the four components in Section 2.

4.2. Internal stability criterion

Now we are ready to present the first theorem on the internal stability region.

Theorem 1. *Consider a platoon of connected vehicles with dynamics given in* (1)*, formation geometry given in* (8)*, and distributed controller given in* (5)*. Suppose that Assumption 1 and Assumption 2 hold and there are no parameter mismatches and disturbances. Then, the platoon is asymptotically stable if and only if*

$$\begin{cases} k_{ip} > 0, \\ k_{ia} > -\frac{1}{r_i}, \\ k_{iv} > k_{ip}(\frac{\tau_i}{1+k_{ia}r_i} - h_i), \end{cases} \quad \forall i \in \mathcal{N}. \tag{12}$$

PROOF. We only need to analyze the stability of the matrix $\tilde{A}$ given in (11). Since $\tilde{A}$ is stable (or Hurwitz) if and only if all of its eigenvalues, denoted by λ_i, have negative real parts. We consider the characteristic equation of $\tilde{A}$.

$$\begin{aligned}
|\lambda I_{3N} - \tilde{A}| &= \begin{vmatrix} \lambda I_N & -I_N & -H \\ 0 & \lambda I_N & -I_N \\ \Delta K_p \mathcal{L}_\mathcal{P} & \Delta K_v \mathcal{L}_\mathcal{P} & \lambda I_N + \Delta + \Delta K_a \mathcal{L}_\mathcal{P} \end{vmatrix} \\
&= \begin{vmatrix} \lambda I_N & -I_N & -H \\ 0 & \lambda I_N & -I_N \\ \Delta K_p \mathcal{L}_\mathcal{P} & \Delta K_v \mathcal{L}_\mathcal{P} & \lambda I_N + \Delta + \Delta K_a \mathcal{L}_\mathcal{P} \end{vmatrix} \begin{vmatrix} I_N & \frac{1}{\lambda} I_N & \frac{1}{\lambda^2} I_N + \frac{1}{\lambda} H \\ 0 & I_N & \frac{1}{\lambda} I_N \\ 0 & 0 & I_N \end{vmatrix} \\
&= \left| \lambda^3 I_N + \lambda^2 \Delta (I_N + K_a \mathcal{L}_\mathcal{P}) + \lambda \Delta (K_v \mathcal{L}_\mathcal{P} + K_p \mathcal{L}_\mathcal{P} H) + \Delta K_p \mathcal{L}_\mathcal{P} \right| \\
&= \prod_{i=1}^{N} \Big(\lambda^3 + \lambda^2 \frac{1}{\tau_i} (1 + k_{ia} r_i) + \lambda \frac{1}{\tau_i} r_i (k_{iv} + k_{ip} h_i) + \frac{1}{\tau_i} r_i k_{ip} \Big).
\end{aligned} \tag{13}$$

The derivation of the last equation in (13) uses the fact that matrices Δ, K_p, K_v, and K_a are diagonal, and matrices $\mathcal{L}_\mathcal{P}$ and H are lower-triangular. The lower-triangular structures of $\mathcal{L}_\mathcal{P}$ and H imposed by the MPF topology make it possible to decouple the system (11) into N subsystems to facilitate the system analysis.

Then, we define the following polynomial

$$p_i(\lambda) := \lambda^3 + \lambda^2 \frac{1}{\tau_i} (1 + k_{ia} r_i) + \lambda \frac{1}{\tau_i} r_i (k_{iv} + k_{ip} h_i) + \frac{1}{\tau_i} r_i k_{ip}. \tag{14}$$

Then, system (11) is stable if and only if the roots of $p_i(\lambda)$ have negative real parts $\forall i \in \mathcal{N}$. Further, according to the Routh-Hurwitz stability criterion, $p_i(\lambda)$ is stable if and only if

$$\begin{cases} \dfrac{1}{\tau_i}(1 + k_{ia} r_i) > 0, \\ \dfrac{1}{\tau_i} r_i (k_{iv} + k_{ip} h_i) > 0, \\ \dfrac{1}{\tau_i} r_i k_{ip} > 0, \\ \Big(\dfrac{1}{\tau_i}(1 + k_{ia} r_i) \Big) \Big(\dfrac{1}{\tau_i} r_i (k_{iv} + k_{ip} h_i) \Big) > \dfrac{1}{\tau_i} r_i k_{ip}. \end{cases} \tag{15}$$

Since $r_i \geq 1 > 0$ and $\tau_i > 0$, the last inequality implies the second one, then we have the following equivalent conditions

$$\begin{gathered}
\frac{1}{\tau_i}(1 + k_{ia} r_i) > 0 \Longleftrightarrow k_{ia} > -\frac{1}{r_i}, \\
\frac{1}{\tau_i} r_i k_{ip} > 0 \Longleftrightarrow k_{ip} > 0, \\
\Big(\frac{1}{\tau_i}(1 + k_{ia} r_i) \Big) \Big(\frac{1}{\tau_i} r_i (k_{iv} + k_{ip} h_i) \Big) > \frac{1}{\tau_i} r_i k_{ip} \Longleftrightarrow k_{iv} > k_{ip} \Big(\frac{\tau_i}{1 + k_{ia} r_i} - h_i \Big).
\end{gathered}$$

To sum up, (15) is equivalent to (12). This completes the proof.

□

Remark 1. The last inequality of (12) can be reduced to

$$h_i > h_{\min,1} := \frac{\tau_i}{1 + k_{ia} r_i} - \frac{k_{iv}}{k_{ip}},$$

which means that h_i should be lower bounded by $h_{\min,1}$. In particular, when $k_{iv} = 0$, $h_{\min,1}$ becomes positive, indicating that without direct velocity error feedback, the minimum employable time headway should be positive, thus the CS policy (where $h_i = 0$) is no longer employable. In addition, when $k_{iv} = k_{ia} = 0$, $h_{\min,1}$ equals τ_i, meaning that the time headway h_i should be greater than the time lag τ_i if there is no direct velocity error and acceleration error feedback. When $h_i = 0$, Theorem 1 is reduced to the case of the CS policy; see (Zheng et al., 2016, 2019) for details.

5. String stability analysis

In this section, we analyze the string stability for a homogeneous platoon based on the following assumption, which is used in (Darbha et al., 2017, 2018).

Assumption 3. The platoon is assumed to be homogenous. In particular, the vehicles have identical time lags, time headways, and control gains, *i.e.*, $\tau_i = \tau > 0$, $h_i = h \geq 0$, $k_{i\sharp} = k_\sharp$, $\sharp \in \{p, v, a\}$, $\forall i \in \mathcal{N}$. The numbers of predecessors are identical, *i.e.*, $r_i = r \geq 1$ if $i \geq r$, and $r_i = i$ if $1 \leq i < r$.

Under Assumption 3, we denote by K_0, K_1, and K_2 the feasible region of $k = [k_p, k_v, k_a]^\top$ that ensures internal asymptotic stability given by Theorem 1, *i.e.*,

$$K_0 := \Big\{ k_a \Big| k_a > -\frac{1}{r} \Big\}, \tag{16a}$$

$$K_1 := \{(k_p, k_v) | k_p > 0\}, \tag{16b}$$

$$K_2 := \Big\{ (k_p, k_v) \Big| k_v - \Big(\frac{\tau}{1 + k_a r} - h \Big) k_p > 0 \Big\}. \tag{16c}$$

Next, we formulate the transfer function of the spacing errors and then present the string stability criterion.

5.1. Transfer function of spacing errors

We consider the amplification of spacing errors since spacing errors directly affect platoon safety. We define the spacing error as $e_i = p_i - p_{i-1} + d_i + h v_i$. According to (1), we know

$$u_i = \tau_i \dot{a}_i + a_i = \tau \dddot{p}_i + \ddot{p}_i.$$

Then from (5), we have

$$\tau \dddot{p}_i + \ddot{p}_i = -\sum_{l=1}^{r} \left(k_p \Big(p_i - p_{i-l} + \sum_{k=i-l+1}^{i} (h v_k + d_k) \Big) + k_v (v_i - v_{i-l}) + k_a (a_i - a_{i-l}) \right), \tag{17}$$

and

$$\tau \dddot{p}_{i-1} + \ddot{p}_{i-1} = -\sum_{l=1}^{r} \left(k_p \Big(p_{i-1} - p_{i-1-l} + \sum_{k=i-l}^{i-1} (h v_k + d_k) \Big) + k_v (v_{i-1} - v_{i-l-1}) + k_a (a_{i-1} - a_{i-l-1}) \right). \tag{18}$$

In addition, the time derivative of (17) is

$$\tau \ddot{v}_i + \ddot{v}_i = -\sum_{l=1}^{r} \left(k_p \Big(v_i - v_{i-l} + \sum_{k=i-l+1}^{i} (h a_k) \Big) + k_v (a_i - a_{i-l}) + k_a (\dot{a}_i - \dot{a}_{i-l}) \right). \tag{19}$$

By calculating (17) − (18) + $h \times$ (19), we have

$$\tau \ddot{e}_i + (r k_a + 1) \ddot{e}_i + r(k_v + k_p h) \dot{e}_i + r k_p e_i = \sum_{l=1}^{r} \left(k_a \ddot{e}_{i-l} + \Big(k_v - k_p h (r - l) \Big) \dot{e}_{i-l} + k_p e_{i-l} \right). \tag{20}$$

With zero initial conditions, the Laplace transform of (20) becomes

$$E_i(s) = \sum_{l=1}^{r} H_l(s) E_{i-l}(s),$$

where $E_i(s)$ is the Laplace transformation of $e_i(t)$, and

$$H_l(s) = \frac{k_a s^2 + \big(k_v - k_p h (r - l) \big) s + k_p}{\tau s^3 + (r k_a + 1) s^2 + r(k_v + k_p h) s + r k_p}.$$

Remark 2. The above approach for transfer function formulation was also used in (Darbha et al., 2017, 2018). Note that the stability of $H_l(s)$ requires that the denominator is Hurwitz. By comparing the denominator with $p_i(\lambda)$ defined in (14), we know that this is equivalent to the internal stability criterion given in Theorem 1.

5.2. String stability criterion

In a MPF topology, the spacing error of vehicle i is affected by its multiple predecessors. We therefore consider the following definition of strictly L_2 string stability:

$$\|e_i(t)\|_2^2 \leq \frac{1}{r}\sum_{l=1}^{r}\|e_{i-l}(t)\|_2^2, \tag{21}$$

where $\|e_i(t)\|_2^2 := \int_{-\infty}^{+\infty}|e_i(t)|^2\mathrm{d}t$ is the L_2 norm of $e_i(t)$. According to (21), it is required that the L_2 spacing error is attenuated in the sense that it is less than the average of its predecessors' L_2 spacing errors. Consider the following *string stability specification* used in (Darbha et al., 2017):

$$\sum_{l=1}^{r}\|H_l(j\omega)\|_\infty \leq 1. \tag{22}$$

Then we have the following two lemmas about the string stability specification.

Lemma 1. *The string stability specification* (22) *is a sufficient condition for the strictly L_2 string stability* (21)*.*

Proof. According to the Parseval's theorem (Arfken & Weber, 1972), we have:

$$\begin{aligned}\|e_i(t)\|_2^2 &= \int_{-\infty}^{+\infty}|e_i(t)|^2\mathrm{d}t\\ &= \frac{1}{2\pi}\int_{-\infty}^{+\infty}|E_i(j\omega)|^2\mathrm{d}\omega\\ &= \frac{1}{2\pi}\int_{-\infty}^{+\infty}\left|\sum_{l=1}^{r}\big(H_l(j\omega)E_{i-l}(j\omega)\big)\right|^2\mathrm{d}\omega.\end{aligned}$$

According to the Cauchy-Schwarz inequality (Steele, 2004), we have

$$\begin{aligned}\|e_i(t)\|_2^2 &\leq \frac{1}{2\pi}\int_{-\infty}^{+\infty}\left(r\sum_{l=1}^{r}\Big(E_{i-l}^{\mathrm{H}}(j\omega)H_l^{\mathrm{H}}(j\omega)H_l(j\omega)E_{i-l}(j\omega)\Big)\right)\mathrm{d}\omega\\ &\leq r\sum_{l=1}^{r}\left(\sup_\omega|H_l(j\omega)|^2\cdot\frac{1}{2\pi}\int_{-\infty}^{+\infty}\Big(E_{i-l}^{\mathrm{H}}(j\omega)E_{i-l}(j\omega)\Big)\mathrm{d}\omega\right)\\ &= r\sum_{l=1}^{r}\Big(\|H_l(j\omega)\|_\infty^2\cdot\|e_{i-l}(t)\|_2^2\Big).\end{aligned} \tag{23}$$

Since $\lim_{\omega\to 0^+}|H_l(j\omega)| = \frac{1}{r}$, we know that (22) holds if and only if

$$\|H_l(j\omega)\|_\infty \leq \frac{1}{r}, \forall 1 \leq l \leq r. \tag{24}$$

Then, when (22) holds, substituting (24) into (23) yields (21). This completes the proof.

□

In particular, when $r = 1$, (22) becomes a necessary and sufficient condition for strictly L_2 string stability (Ploeg et al., 2014a).

Lemma 2. *The string stability specification* (22) *holds if and only if either one of the following conditions holds for both cases when $l = 1$ and $l = r$:*

$$C_0 \geq 0 \quad\wedge\quad C_1 \geq 0, \tag{25a}$$

$$C_0 \geq 0 \quad\wedge\quad C_1 < 0 \quad\wedge\quad \Delta_{\mathrm{d}} \leq 0, \tag{25b}$$

where

$$\Delta_{\rm d} := C_1^2 - 4C_2C_0, \tag{26a}$$

$$C_2 := \tau^2, \tag{26b}$$

$$C_1 := 2k_a r + 1 - 2r\tau(k_v + hk_p), \tag{26c}$$

$$C_0 := k_p r\Big(r\big(1-(l-r)^2\big)h^2k_p + 2r(1+r-l)hk_v - 2\Big). \tag{26d}$$

PROOF. According to (24), we know that (22) holds if and only if

$$\max_{1\le l\le r}\|H_l(j\omega)\|_\infty^2 = \max_{1\le l\le r}\sup_{\omega>0}|H_l(j\omega)|^2 = \max\Big\{\sup_{\omega>0}|H_1(j\omega)|^2, \sup_{\omega>0}|H_r(j\omega)|^2\Big\} \le \frac{1}{r^2}, \tag{27}$$

where

$$|H_l(j\omega)|^2 := \frac{N_l}{D_l} = \frac{(k_p - k_a\omega^2)^2 + \big(k_v - k_p h(r-l)\big)^2\omega^2}{\big(r(k_v+k_ph)\omega - \tau\omega^3\big)^2 + \big(rk_p - (rk_a+1)\omega^2\big)^2}.$$

The derivation of the last equation in (27) uses the fact that $|H_l(j\omega)|^2$ is a quadratic function of l. Then we know that the inequality in (27) holds if and only if

$$D_l - r^2N_l = \omega^2\big(C_2\omega^4 + C_1\omega^2 + C_0\big) \ge 0, \forall l \in \{1, r\}, \tag{28}$$

where C_2, C_1, and C_0 are defined as (26b), (26c), and (26d), respectively. Then we only need to consider the bi-quadratic function $C_2w^4 + C_1w^2 + C_0$, of which the discriminant is $\Delta_{\rm d}$ defined in (26a). Since $C_2 > 0$, we know that (28) holds if and only if $\forall l \in \{1, r\}$, (25a) or (25b) holds. This completes the proof.

□

Then, we are ready to present the second theorem about the string stability criterion.

Theorem 2. *Consider a platoon of connected vehicles with dynamics given in* (1)*, formation geometry given in* (8)*, and distributed controller given in* (5)*. Suppose that Assumption 1 and Assumption 3 hold and there are no parameter mismatches and disturbances. Then, there exists a set of feedback gains* $k = [k_p, k_v, k_a]^\top$ *such that the string stability specification* (22) *holds if and only if:*

$$h \ge h_{\min,2} := \frac{2\tau}{2k_ar+1}, k_a > -\frac{1}{2r}. \tag{29}$$

PROOF. The proof is based on the analysis of the region defined in (25). See the Appendix for details. □

According to Theorem 2, increasing k_a or r (when $k_a > 0$) can reduce the bound $h_{\min,2}$, which implies a lower inter-vehicle distance and higher traffic capacity. The bound $h_{\min,2}$ remains unchanged when there is no acceleration feedback (*i.e.*, $k_a = 0$). In this case, Theorem 2 is consistent with the result in (Darbha & Rajagopal, 2001), which indicates that the employable time headway is lower bounded by 2τ for string stability. For ACC systems that do not have V2V communication capability, only one predecessor's information is available (*i.e.*, $r = 1$), then the only way to reduce $h_{\min,2}$ is to increase k_a. In this case, Theorem 2 agrees with the result in (Darbha et al., 2017, 2018). Note that our result extends (Darbha et al., 2017, 2018) by considering a new CTH policy to avoid inconsistency in desired inter-vehicle distances. Theorem 2 is based on the assumption of a homogeneous platoon. Still, simulations with a heterogeneous platoon in Section 6.2 suggest that the results are useful and might provide certain guidelines for heterogeneous platoons.

When actuator delays exist, the third equation in vehicle dynamics (1) becomes $\tau_i\dot{a}_i(t) + a_i(t) = u_i(t - \tau_{\rm a})$, where $\tau_{\rm a} > 0$ is the actuator delay. Then, as suggested by (Xiao & Gao, 2011), an intuition is that $h_{\min,2}$ may be increased to $\frac{2(\tau+\tau_{\rm a})}{2k_ar+1}$. However, this intuition needs a theoretical proof, which is out of the scope of this paper.

Remark 3. For Theorem 1, the exact value of τ_i is not required for the design of h_i and $k_i = [k_{ip}, k_{iv}, k_{ia}]^\top$, as long as there exists a known upper bound of τ_i. For Theorem 2, the design of $h_i = h$ needs the upper bound of $\tau_i = \tau$, while the design of $k_i = k = [k_p, k_v, k_a]^\top$ needs both the upper and lower bounds of τ when calculating the sets K_i, $i \in \{1, 2, .., 8\}$ defined in (34a)-(34f). This is consistent with the notion of robust string stability in (Darbha et al., 2018).

From Theorem 2, we can easily get the following corollary, which is consistent with the results in (Seiler et al., 2004; Naus et al., 2010; Konduri et al., 2017).

Corollary 1. *Consider a platoon of connected vehicles with dynamics given in* (1)*, formation geometry given in* (8)*, and distributed controller given in* (5)*. Suppose that Assumption 1 and Assumption 3 hold and there are no parameter mismatches and disturbances. Then, if the formation geometry uses the CS policy, i.e.,* $h = 0$*, the string stability specification* (22) *will not hold. Consequently, the platoon can never be string stable for any feedback gains when* $r = 1$*.*

6. Numerical experiments

This section presents numerical simulations to validate the proposed theorems. According to (21), we use the following performance index to evaluate the attenuation of spacing errors

$$Q_i := \frac{r\|e_i(t)\|_2^2}{\sum_{l=1}^{r}\|e_{i-l}(t)\|_2^2}, i \in \{r+1, r+2, \ldots, N\}.$$

Then we know $Q_i \leq 1, \forall i \in \{r+1, r+2, \ldots, N\}$ when the platoon is string stable. On the contrary, if $\exists i \in \{r+1, r+2, \ldots, N\}$ such that $Q_i > 1$, the platoon is string unstable. In addition, both the nominal linear vehicle model (1) and a realistic nonlinear vehicle model, given in (30), are used for validation. Throughout this section, we plotted spacing error profiles of all vehicles in the figures, but only the legends of odd numbered vehicles were given due to space limit.

6.1. Simulations of linear platoons

First, we validate the proposed theorems by simulations with the nominal linear vehicle model (1). We consider platoon control in three cases, *i.e.*, 1) $h \leq h_{\min,1}$, 2) $h_{\min,1} < h \leq h_{\min,2}$, and 3) $h > h_{\min,2}$, and the number of predecessors is $r = 1$ or $r = 3$. The initial errors are assumed to be zero, and a sinusoidal input disturbance $u_{\mathrm{d}} = A_{\mathrm{d}} \sin\big(\omega_{\mathrm{d}}(t-5)\big)$ is imposed on the leading vehicle during the time period $5 \leq t \leq 5 + \frac{2\pi}{\omega_{\mathrm{d}}}$ (s). The simulation parameters are listed in Table 1 and simulation results are shown in Figure 2, Figure 3, and Table 2.

As shown in Figure 2(d) and Figure 3(d), when $h \leq h_{\min,1}$, there are peaks in the magnitude-frequency diagrams, which correspond to the poles of $H_l(j\omega)$. In this case, the platoons are not stable, which confirms Theorem 1. As shown in Figure 2(e) and Figure 3(e), when $h_{\min,1} < h \leq h_{\min,2}$, the magnitude of $H_l(j\omega)$ surpasses $\frac{1}{r}$, which means (22) does not hold. Besides, the spacing errors converge to zero when the disturbances are removed. As shown in Table 2, when $r = 1$, we have $Q_i > 1$, $\forall i \in \{2, 3, \ldots, 7\}$, so the platoon is asymptotically stable but not string stable. This agrees with Theorem 2. Besides, it is observed that $Q_i < 1$, $\forall i \in \{4, 5, 6, 7\}$ when $r = 3$ and $h_{\min,1} < h \leq h_{\min,2}$. This is because that $E_{i-1}(s)$, $E_{i-2}(s)$ and $E_{i-3}(s)$ have different phases, so their effects on $E_i(s)$ cancel out each other.

As shown in Figure 2(f) and Figure 3(f), when $h > h_{\min,2}$, the magnitude of $H_l(j\omega)$ does not surpass $\frac{1}{r}$, which means (22) holds. Besides, the spacing errors converge to zero when the disturbances are removed. As shown in Table 2, we have $Q_i < 1$, $\forall i \in \{r+1, r+2, \ldots, 7\}$. This demonstrates that the platoons are both asymptotically stable and string stable, which confirms Theorem 2.

In Figure 3(b) and Figure 3(c), it is observed that the phase of $e_1(t)$ is opposite to those of the other vehicles, which is different from the case in Figure 2(b) and Figure 2(c). This phenomenon arises from the MPF topology and the CTH policy. At $t = 5$ (s) when vehicle 0 starts to accelerate, since vehicle 1, 2, and 3 are all connected to vehicle 0, the term $p_{ii}(k_{ip}\tilde{p}_i + k_{iv}\tilde{v}_i + k_{ia}\tilde{a}_i)$ dominates their feedback inputs in (5), so they all start to accelerate, and v_1, v_2, and v_3 start to increase. However, the increase of $p_0 - p_1$ is greater than that of $p_1 - p_2$, $p_2 - p_3$, and hv_1, so $e_1 = -(p_0 - p_1) + d_1 + hv_1$ becomes negative, while $e_2 = -(p_1 - p_2) + d_2 + hv_2$ and $e_3 = -(p_2 - p_3) + d_3 + hv_3$ become positive, which causes the opposite phases. When it comes to vehicle 4, since it is not connected to vehicle 0, the increase of v_4 is lower than that of v_1, v_2, and v_3. In addition, $p_3 - p_4$ and hv_4 are almost at the same scale, so $e_4 = -(p_3 - p_4) + d_4 + hv_4$ is very close to 0. This also explains why Q_4 is very close to zero. The behaviors of vehicles 5, 6, and 7 are similar to those of vehicles 2 and 3.

Table 1: Simulation parameters of linear platoons

Model parameters		
Parameter	Unit	Value
N	-	7
A_{d}	[m/s^2]	1
d_i	[m]	10
v_0	[m/s]	20
τ	[s]	0.50

Control parameters								
Figure	r	k_p	k_v	k_a	ω_{d} [rad/s]	$h_{\mathrm{min},1}$ [s]	$h_{\mathrm{min},2}$ [s]	h [s]
4(a)	1	0.1	0.01	0.01	1.0	0.395	0.980	0.316
4(b)	1	0.1	2.51	0.51	1.0	-24.7	0.495	0.396
4(c)	1	0.1	1.65	0.51	1.0	-16.2	0.495	0.594
5(a)	3	0.1	0.01	0.68	1.6	0.065	0.198	0.052
5(b)	3	0.1	2.52	0.84	1.6	-25.0	0.165	0.132
5(c)	3	0.1	1.67	0.84	1.6	-16.6	0.165	0.198

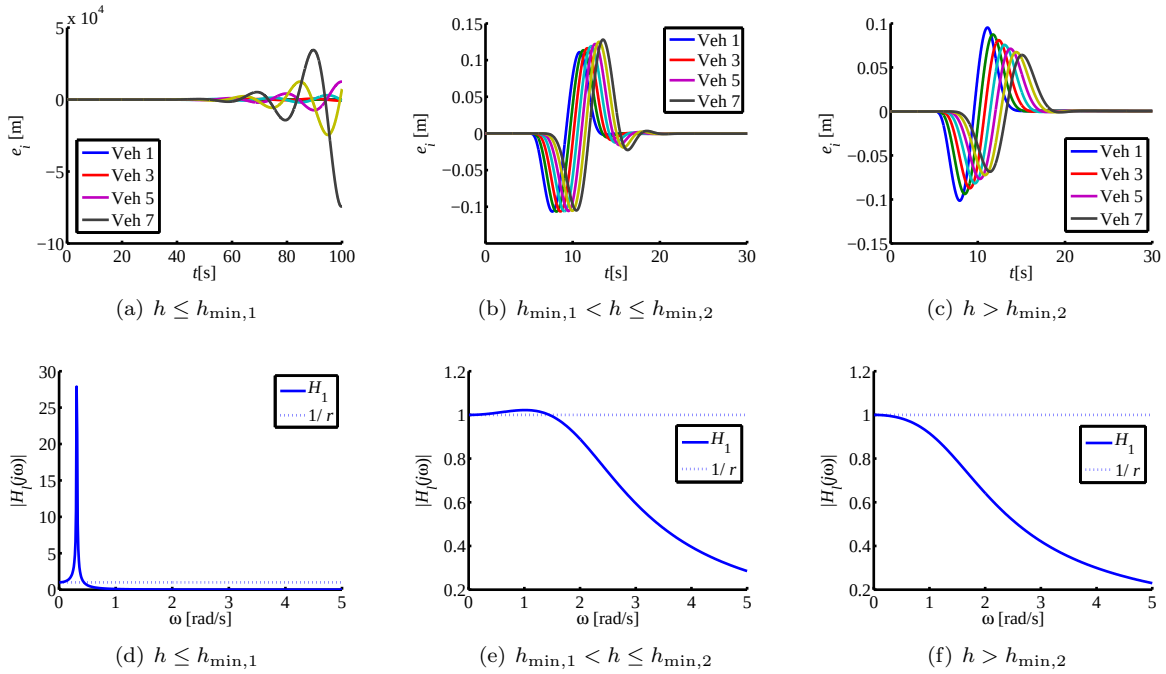

(a) $h \le h_{\mathrm{min},1}$ (b) $h_{\mathrm{min},1} < h \le h_{\mathrm{min},2}$ (c) $h > h_{\mathrm{min},2}$

(d) $h \le h_{\mathrm{min},1}$ (e) $h_{\mathrm{min},1} < h \le h_{\mathrm{min},2}$ (f) $h > h_{\mathrm{min},2}$

Figure 2: Simulation results of linear platoons ($r = 1$)

Table 2: Performance index of linear platoons

Figure	r	Q_2	Q_3	Q_4	Q_5	Q_6	Q_7
2(b)	1	1.031	1.032	1.033	1.033	1.033	1.034
2(c)	1	0.890	0.900	0.908	0.915	0.921	0.926
3(b)	3	-	-	0.007	0.635	0.601	0.621
3(c)	3	-	-	0.000	0.636	0.601	0.608

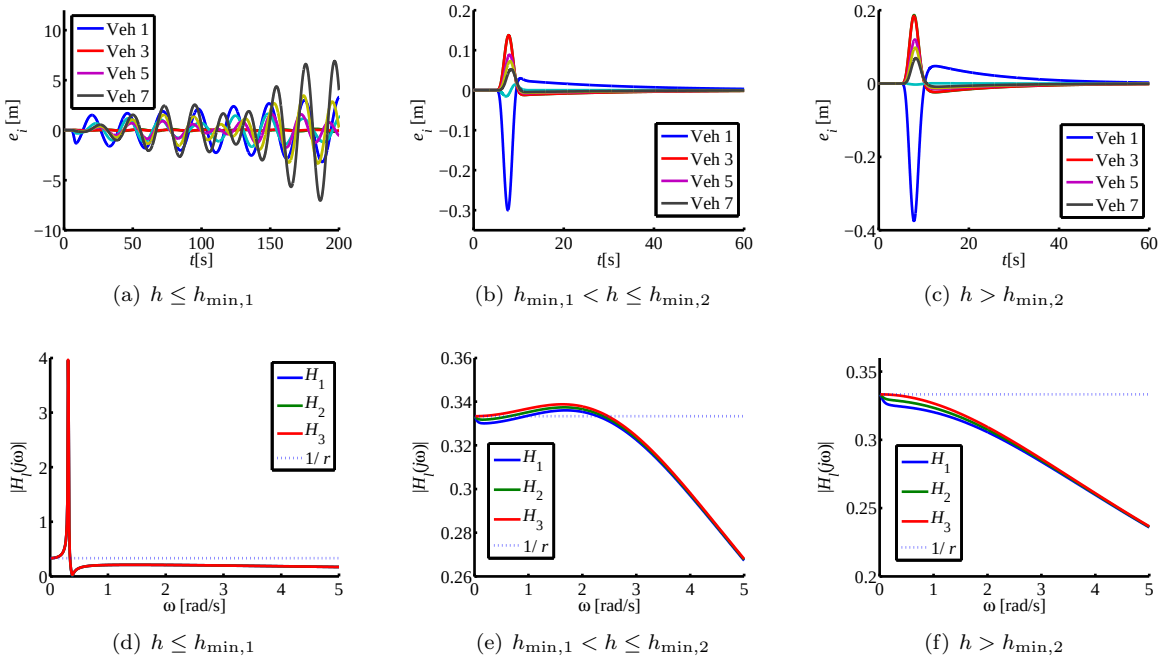

(a) $h \le h_{\min,1}$ (b) $h_{\min,1} < h \le h_{\min,2}$ (c) $h > h_{\min,2}$

(d) $h \le h_{\min,1}$ (e) $h_{\min,1} < h \le h_{\min,2}$ (f) $h > h_{\min,2}$

Figure 3: Simulation results of linear platoons ($r = 3$)

6.2. Simulations of nonlinear platoons

Next, we evaluate the effectiveness of the proposed theorems for realistic nonlinear platoons. We consider the following nonlinear vehicle model, which is also used in (Dunbar & Caveney, 2012; Kwon & Chwa, 2014):

$$\begin{cases} \dot{p}_i = v_i, \\ m_i \dot{v}_i = \frac{\eta_i}{r_i} T_i - C_{\mathrm{A},i} v_i^2 - m_i g f_i, \quad i \in \{0\} \cup \mathcal{N}, \\ \tau_i \dot{T}_i + T_i = T_{\mathrm{des},i}, \end{cases} \tag{30}$$

where $T_{\mathrm{des},i}$, T_i, and η_i are the desired driving torque (control input), the actual driving torque, and the mechanical efficiency of the driveline, respectively; m_i and r_i are the mass and tire radius, respectively; $C_{\mathrm{A},i}$, f_i, and g are the coefficients of the aerodynamic drag, rolling resistance, and gravitational acceleration, respectively.

For nonlinear model (30), we use the following feedback linearization law, which is also used in (Xiao & Gao, 2011; Ghasemi et al., 2013):

$$T_{\mathrm{des},i} = \frac{\hat{r}_i}{\hat{\eta}_i} (\hat{m}_i u_{\mathrm{r},i} + \hat{f}_i \hat{m}_i g + 2\hat{C}_{\mathrm{A},i} \hat{\tau}_i v_i a_i + \hat{C}_{\mathrm{A},i} v_i^2),$$

where $\hat{m}_i$, $\hat{\eta}_i$, $\hat{r}_i$, $\hat{C}_{\mathrm{A},i}$, $\hat{f}_i$, and $\hat{\tau}_i$ are the estimations of m_i, η_i, r_i, $C_{\mathrm{A},i}$, f_i, and τ_i, respectively; $u_{\mathrm{r},i}$ is the robust control input, which is obtained by adding a non-smooth term to the nominal control input u_i given in (5) to compensate the parameter mismatch:

$$u_{\mathrm{r},i} = u_i - k_{\mathrm{s},i} \mathrm{sign}(s_i), \tag{31}$$

where $k_{\mathrm{s},i}$ is the feedback gain, $\mathrm{sign}(\cdot)$ is the sign function, and s_i is the integral sliding mode variable, of which the derivative is:

$$\dot{s}_i = \hat{\tau}_i \dot{a}_i + a_i - u_i,$$

and the integral initial value is zero. This robust controller is designed based on the integral sliding mode control theory (Utkin et al., 2009) and is also used in (Zheng et al., 2019).

In this simulation, we consider platoon control in the case of $h > h_{\min,2}$, and the number of predecessors is $r = 1$ or $r = 3$. The simulation parameters are listed in Table 3. As shown in Table 3, model parameters take random

values, which are determined by the uniformly distributed random variable $\theta \sim U(0,1)$; therefore, the nonlinear platoons are actually heterogeneous. Moreover, the parameter mismatch from the inaccurate parameter estimation also imposes equivalent disturbances on each vehicle. The simulation results are shown in Figure 4 and Table 4.

As shown in Figure 4, the spacing errors converge to zero when the disturbances are removed. From Table 4, it is observed that $Q_i < 1$, $\forall i \in \{r+1, r+2, \ldots, 7\}$. This means that the nonlinear platoons are still asymptotically stable and string stable even if heterogeneity and parameter mismatch exist.

Table 3: Simulation parameters of nonlinear platoons

Model parameters $[\theta \sim U(0,1)]$			
Parameter	Unit	True value	Estimated value
N	-	7	-
A_{d}	[m/s^2]	1	-
d_i	[m]	10	-
v_0	[m/s]	20	-
τ_i	[s]	$0.40 + 0.20\times\theta$	0.50
m_i	[kg]	$1500 + 400\times\theta$	1700
η_i	-	$0.80 + 0.08\times\theta$	0.84
r_i	-	$0.250 + 0.060\times\theta$	0.28
$C_{\mathrm{A},i}$	[kg/m]	$0.40 + 0.10\times\theta$	0.45
f_i	[m]	$0.015 + 0.006\times\theta$	0.018

Control parameters									
Figure	r	k_p	k_v	k_a	$k_{\mathrm{s},i}$	ω_{d} [rad/s]	$h_{\mathrm{min},1}$ [s]	$h_{\mathrm{min},2}$ [s]	h [s]
4(a)	1	0.1	1.65	0.51	1	1.0	-16.2	0.495	0.594
4(b)	3	0.1	1.67	0.84	1	1.6	-16.6	0.165	0.198

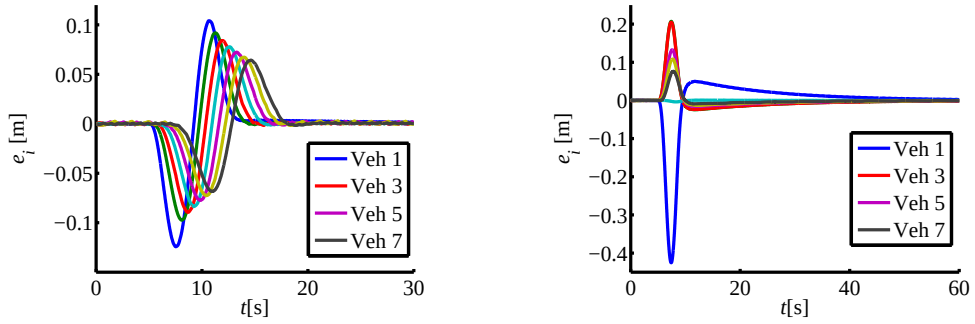

(a) $r = 1$ (b) $r = 3$

Figure 4: Simulation results of nonlinear platoons

Table 4: Performance index of nonlinear platoons

Figure	r	Q_2	Q_3	Q_4	Q_5	Q_6	Q_7
4(a)	1	0.7040	0.8869	0.9015	0.8903	0.9073	0.9256
4(b)	3	-	-	0.0002	0.6325	0.5999	0.6024

6.3. Simulations of nonlinear platoons subject to communication time delays

Then, we evaluate the impact of communication time delays on nonlinear platoons. On the basis of the simulations given in Subsection 6.2, we impose identical communication time delays t_{d} on V2V communications, which

can be measured using communication timestamps. In this case, at time t, vehicle i can only obtain the delayed neighbor states $p_j(t-t_\mathrm{d})$, $v_j(t-t_\mathrm{d})$, and $a_j(t-t_\mathrm{d})$. By assuming that the neighbors have constant acceleration motions, the estimated neighbor states at time t become $\hat{p}_j(t) = p_j(t-t_\mathrm{d}) + v_j(t-t_\mathrm{d})t_\mathrm{d} + \frac{1}{2}a_j(t-t_\mathrm{d})t_\mathrm{d}^2$, $\hat{v}_j(t) = v_j(t-t_\mathrm{d}) + a_j(t-t_\mathrm{d})t_\mathrm{d}$, and $\hat{a}_j(t) = a_j(t-t_\mathrm{d})$. Then, by replacing $[p_j(t), v_j(t), a_j(t)]$ with $[\hat{p}_j(t), \hat{v}_j(t), \hat{a}_j(t)]$ in u_i given in (5), vehicle i continues to use controller $u_{\mathrm{r},i}$ given in (31) for feedback control. In this simulation, we consider platoon control in the case of $h > h_{\min,2}$ and $r = 1$ or 3, and the communication time delay is $t_\mathrm{d} = 100$ ms, 200 ms, 300 ms, or 400 ms. The simulation parameters are the same as Table 3, and simulation results are shown in Figure 5 and Table 5.

As shown in Figure 5, vehicles' position tracking errors increase as the communication time delay increases. As shown in Table 5, when $r = 1$, the nonlinear platoons are string stable if $t_\mathrm{d} \le 200$ ms, but string instable if $t_\mathrm{d} \ge 300$ ms. When $r = 3$, these two thresholds are increased to $t_\mathrm{d} \le 300$ ms and $t_\mathrm{d} \ge 400$ ms. These results show that the platoon string stability can still be guaranteed if the communication time delays are upper bounded. The determination of these bounds in theory deserves further investigations, which is beyond the scope of this work.

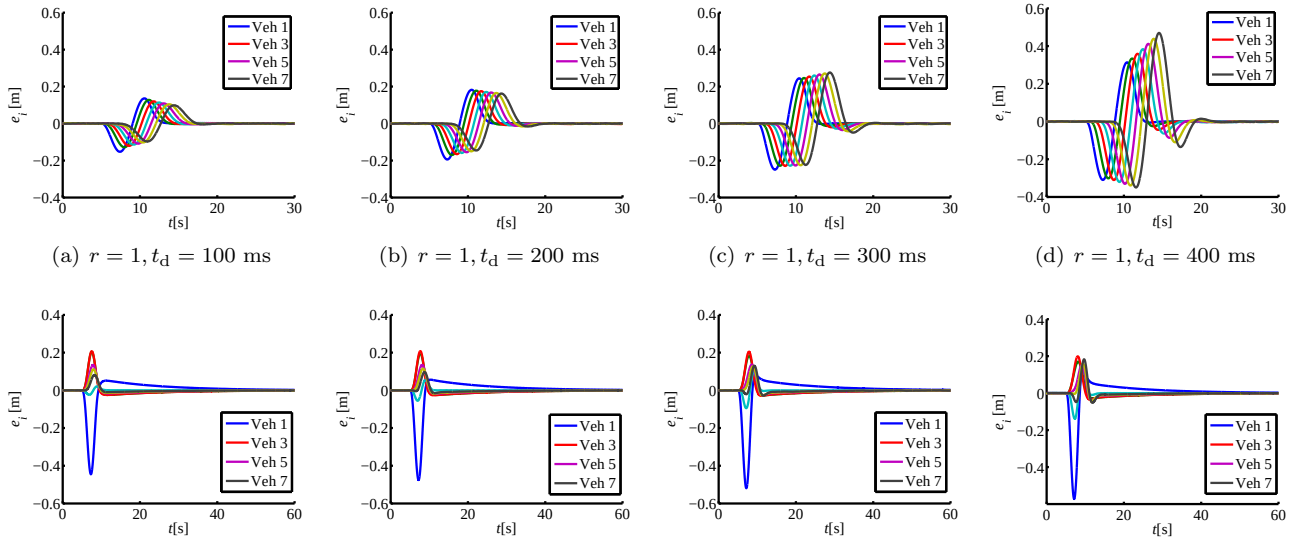

(a) $r = 1, t_\mathrm{d} = 100$ ms (b) $r = 1, t_\mathrm{d} = 200$ ms (c) $r = 1, t_\mathrm{d} = 300$ ms (d) $r = 1, t_\mathrm{d} = 400$ ms

(e) $r = 3, t_\mathrm{d} = 100$ ms (f) $r = 3, t_\mathrm{d} = 200$ ms (g) $r = 3, t_\mathrm{d} = 300$ ms (h) $r = 3, t_\mathrm{d} = 400$ ms

Figure 5: Simulation results of nonlinear platoons

Table 5: Performance index of nonlinear platoons subject to communication time delays

Figure	r	t_d [ms]	Q_2	Q_3	Q_4	Q_5	Q_6	Q_7
5(a)	1	100	0.8027	0.9139	0.9242	0.9363	0.9311	0.9250
5(b)	1	200	0.8665	0.9786	0.9617	0.9789	0.9718	0.9722
5(c)	1	300	0.9333	1.0487	1.0316	1.0334	1.0314	1.0305
5(d)	1	400	1.0440	1.1131	1.1162	1.1273	1.1135	1.1280
5(e)	3	100	-	-	0.0073	0.6315	0.6061	0.6284
5(f)	3	200	-	-	0.0393	0.6466	0.6093	0.7147
5(g)	3	300	-	-	0.1109	0.6394	0.6332	0.8858
5(h)	3	400	-	-	0.2244	0.6578	0.7182	1.1174

6.4. Simulations of large-scale nonlinear platoons

Finally, we evaluate the performance of the proposed methods for large-scale nonlinear platoons. On the basis of the simulations given in Subsection 6.2, we extend the scale of nonlinear platoons to 50 vehicles. The speed profile

of the leading vehicle is given as follows:

$$v_0 = \begin{cases} 20, & 0\,\mathrm{s} \le t < 10\,\mathrm{s}, \\ 20-(t-10), & 10\,\mathrm{s} \le t < 20\,\mathrm{s}, \\ 10, & 20\,\mathrm{s} \le t < 40\,\mathrm{s}, \\ 10+(t-40), & 40\,\mathrm{s} \le t < 50\,\mathrm{s}, \\ 20, & 50\,\mathrm{s} \le t, \end{cases} \quad [\mathrm{m/s}]$$

and no input disturbances are considered. In this simulation, we consider platoon control in the case of $h \ge h_{\min,2}$ and the number of predecessors is $r = 10$, 20, or 30. The model parameters are the same as Table 3, and the control parameters are listed in Table 6. As shown in Table 6, the lower bound of time headway $h_{\min,2}$ is reduced to less than or equal to 0.050 s when $r \ge 10$, which indicates a negligible change of inter-vehicle distances as the traffic flow speed varies.

As shown in Figure 6, the time-space trajectories of the large-scale nonlinear platoons are smooth, and no stop-and-go phenomenon occurs, which indicates a high traffic throughput. Moreover, in these simulations, it holds that $Q_i < 1$, $\forall i \in \{r+1, r+2, \ldots, 50\}$, which demonstrates the string stability for large-scale platoons.

Table 6: Control parameters of large-scale nonlinear platoons

Figure	r	k_p	k_v	k_a	$k_{\mathrm{s},i}$	$h_{\min,1}$ [s]	$h_{\min,2}$ [s]	h [s]
6(a)	10	0.1	1.68	0.96	1	-16.765	0.050	0.059
6(b)	20	0.1	1.68	0.99	1	-16.799	0.025	0.030
6(c)	30	0.1	1.68	0.99	1	-16.810	0.017	0.020

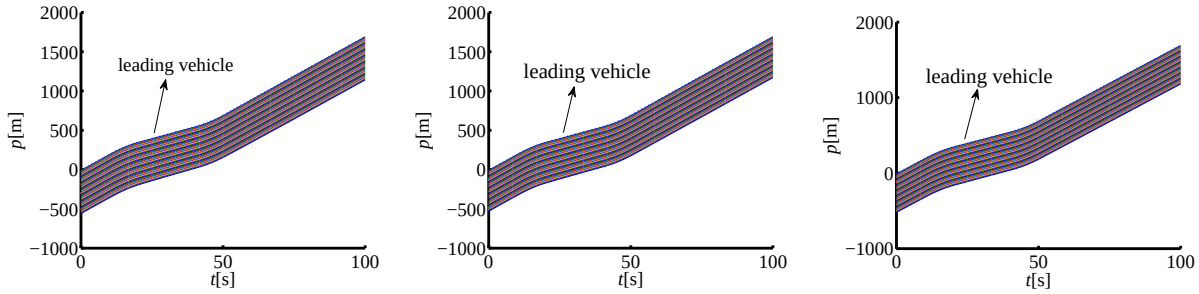

(a) $r = 10$ (b) $r = 20$ (c) $r = 30$

Figure 6: Simulation results of large-scale nonlinear platoons

7. Conclusion

This paper has studied the multiple-predecessor following strategy to reduce time headway for asymptotically stable and string stable platoons via V2V communication. We have proposed a new definition of desired inter-vehicle distances using CTH that avoids inconsistency in desired inter-vehicle distances. With the proposed range policy, we have designed a linear feedback controller and then derived necessary and sufficient conditions for the internal asymptotic stability and the string stability specification. It is proved that there exists a set of feedback gains to ensure the internal asymptotic stability and the string stability specification if and only if the time headway is lower bounded. This finding further indicates that increasing the number of predecessors can reduce the time headway, which, in turn, helps improve transport capacity for highway traffic. As the numerical experiments demonstrated, the string stability of linear and nonlinear platoons can be guaranteed with the proposed methods if the communication time delay is upper bounded. One future work is to directly consider the effect of the heterogeneity on the string stability of vehicular platoons. The effect of communication delays and packet losses is another interesting direction for future studies.

Acknowledgment

This work was supported by National Key R&D Program of China with 2016YFB0100906, NSF China with 51575293 and 51622504, and International Sci&Tech Cooperation Program of China under 2016YFE0102200. Yougang Bian's work was supported in part by the China Scholarship Council.

References

Al-Jhayyish, A. M. H., & Schmidt, K. W. (2018). Feedforward strategies for cooperative adaptive cruise control in heterogeneous vehicle strings. *IEEE Transactions on Intelligent Transportation Systems*, *19*, 113–122. doi:10.1109/TITS.2017.2773659.

Arfken, G. B., & Weber, H.-J. (1972). *Mathematical methods for physicists*. Academic Press New York 1970.

Baldi, S., & Frasca, P. (2018). Adaptive synchronization of unknown heterogeneous agents: An adaptive virtual model reference approach. *Journal of the Franklin Institute*, (pp. 1–21). doi:10.1016/j.jfranklin.2018.01.022.

Barooah, P., & Hespanha, J. P. (2005). Error amplification and disturbance propagation in vehicle strings with decentralized linear control. In *Proceedings of the IEEE Conference on Decision and Control/European Control Conference* (pp. 4964–4969). doi:10.1109/CDC.2005.1582948.

di Bernardo, M., Salvi, A., & Santini, S. (2015). Distributed consensus strategy for platooning of vehicles in the presence of time-varying heterogeneous communication delays. *IEEE Transactions on Intelligent Transportation Systems*, *16*, 102–112. doi:10.1109/TITS.2014.2328439.

Besselink, B., & Johansson, K. H. (2017). String stability and a delay-based spacing policy for vehicle platoons subject to disturbances. *IEEE Transactions on Automatic Control*, *62*, 4376–4391. doi:10.1109/TAC.2017.2682421.

Bian, Y., Zheng, Y., Li, S. E., Wang, Z., Xu, Q., Wang, J., & Li, K. (2018). Reducing time headway for platoons of connected vehicles via multiple-predecessor following. In *Prodeedings of the IEEE International Conference on Intelligent Transportation Systems* (pp. 1240–1245). doi:10.1109/ITSC.2018.8569652.

Cao, Y., & Ren, W. (2012). Distributed coordinated tracking with reduced interaction via a variable structure approach. *IEEE Transactions on Automatic Control*, *57*, 33–48. doi:10.1109/TAC.2011.2146830.

Chehardoli, H., & Ghasemi, A. (2018). Adaptive centralized/decentralized control and identification of 1-D heterogeneous vehicular platoons based on constant time headway policy. *IEEE Transactions on Intelligent Transportation Systems*, (pp. 1–11). doi:10.1109/TITS.2017.2781152.

Chehardoli, H., & Homaeinezhad, M. R. (2017). Third-order safe consensus of heterogeneous vehicular platoons with MPF network topology: Constant time headway strategy. *Proceedings of the Institution of Mechanical Engineers, Part D: Journal of Automobile Engineering*, (pp. 1–12). doi:10.1177/0954407017729309.

Darbha, S., & Hedrick, J. (1999). Constant spacing strategies for platooning in Automated Highway Systems. *Journal of Dynamic Systems Measurement and Control-Transactions of the ASME*, *121*, 462–470. doi:10.1115/1.2802497.

Darbha, S., Konduri, S., & Pagilla, P. R. (2017). Effects of V2V communication on time headway for autonomous vehicles. In *Proceedings of the American Control Conference* (pp. 2002–2007). doi:10.23919/ACC.2017.7963246.

Darbha, S., Konduri, S., & Pagilla, P. R. (2018). Benefits of V2V communication for autonomous and connected vehicles. *IEEE Transactions on Intelligent Transportation Systems*, (pp. 1–10). doi:10.1109/TITS.2018.2859765.

Darbha, S., & Rajagopal, K. (2001). A review of constant time headway policy for automatic vehicle following. In *Proceedings of the IEEE Intelligent Transportation Systems* (pp. 65–69). doi:10.1109/ITSC.2001.948631.

Dunbar, W. B., & Caveney, D. S. (2012). Distributed receding horizon control of vehicle platoons: Stability and string stability. *IEEE Transactions on Automatic Control*, *57*, 620–633. doi:10.1109/TAC.2011.2159651.

Fax, J., & Murray, R. (2004). Information flow and cooperative control of vehicle formations. *IEEE Transactions on Automatic Control*, *49*, 1465–1476. doi:10.1109/TAC.2004.834433.

Flores, C., & Milanés, V. (2018). Fractional-order-based ACC/CACC algorithm for improving string stability. *Transportation Research Part C: Emerging Technologies*, *95*, 381–393. doi:10.1016/j.trc.2018.07.026.

Ge, J. I., & Orosz, G. (2014). Dynamics of connected vehicle systems with delayed acceleration feedback. *Transportation Research Part C: Emerging Technologies*, *46*, 46–64. doi:10.1016/j.trc.2014.04.014.

Ge, J. I., & Orosz, G. (2018). Connected cruise control among human-driven vehicles: Experiment-based parameter estimation and optimal control design. *Transportation Research Part C: Emerging Technologies*, *95*, 445–459. doi:10.1016/j.trc.2018.07.021.

Ghasemi, A., Kazemi, R., & Azadi, S. (2013). Stable decentralized control of a platoon of vehicles with heterogeneous information feedback. *IEEE Transactions on Vehicular Technology*, *62*, 4299–4308. doi:10.1109/TVT.2013.2253500.

Guo, X., Wang, J., Liao, F., & Teo, R. S. H. (2016). Distributed adaptive integrated-sliding-mode controller synthesis for string stability of vehicle platoons. *IEEE Transactions on Intelligent Transportation Systems*, *17*, 2419–2429. doi:10.1109/TITS.2016.2519941.

Harfouch, Y. A., Yuan, S., & Baldi, S. (2018). An adaptive switched control approach to heterogeneous platooning with intervehicle communication losses. *IEEE Transactions on Control of Network Systems*, *5*, 1434–1444. doi:10.1109/TCNS.2017.2718359.

Jadbabaie, A., Lin, J., & Morse, A. (2003). Coordination of groups of mobile autonomous agents using nearest neighbor rules. *IEEE Transactions on Automatic Control*, *48*, 988–1001. doi:10.1109/TAC.2003.812781.

Khatir, M., & Davison, E. (2004). Bounded stability and eventual string stability of a large platoon of vehicles using non-identical controllers. In *Proceedings of the IEEE Conference on Decision and Control* (pp. 1111–1116). doi:10.1109/CDC.2004.1428841.

Konduri, S., Pagilla, P. R., & Darbha, S. (2017). Vehicle platooning with multiple vehicle look-ahead information. *IFAC Papersonline*, *50*, 5768–5773. doi:10.1016/j.ifacol.2017.08.415.

Kwon, J.-W., & Chwa, D. (2014). Adaptive bidirectional platoon control using a coupled sliding mode control method. *IEEE Transactions on Intelligent Transportation Systems*, *15*, 2040–2048. doi:10.1109/TITS.2014.2308535.

Li, S. E., Qin, X., Zheng, Y., Wang, J., Li, K., & Zhang, H. (2017a). Distributed platoon control under topologies with complex eigenvalues: Stability analysis and controller synthesis. *IEEE Transactions on Control Systems Technology*, (pp. 1–15). doi:10.1109/TCST.2017.2768041.

Li, S. E., Zheng, Y., Li, K., & Wang, J. (2015). An overview of vehicular platoon control under the four-component framework. In *Proceedings of the IEEE Intelligent Vehicles Symposium* (pp. 286–291). doi:10.1109/ivs.2015.7225700.

Li, S. E., Zheng, Y., Li, K., Wu, Y., Hedrick, J. K., Gao, F., & Zhang, H. (2017b). Dynamical modeling and distributed control of connected and automated vehicles: Challenges and opportunities. *IEEE Intelligent Transportation Systems Magazine*, *9*, 46–58. doi:10.1109/MITS.2017.2709781.

Lioris, J., Pedarsani, R., Tascikaraoglu, F. Y., & Varaiya, P. (2017). Platoons of connected vehicles can double throughput in urban roads. *Transportation Research Part C: Emerging Technologies*, *77*, 292–305. doi:10.1016/j.trc.2017.01.023.

Milanés, V., Marouf, M., Prez, J., Gonzlez, D., & Nashashibi, F. (2014a). Low-speed cooperative car-following fuzzy controller for cybernetic transport systems. In *Proceedings of the IEEE International Conference on Intelligent Transportation Systems* (pp. 2075–2080). doi:10.1109/ITSC.2014.6958009.

Milanés, V., Shladover, S. E., Spring, J., Nowakowski, C., Kawazoe, H., & Nakamura, M. (2014b). Cooperative adaptive cruise control in real traffic situations. *IEEE Transactions on Intelligent Transportation Systems*, *15*, 296–305. doi:10.1109/TITS.2013.2278494.

Naus, G. J. L., Vugts, R. P. A., Ploeg, J., van de Molengraft, M. R. J. G., & Steinbuch, M. (2010). String-stable CACC design and experimental validation: A frequency-domain approach. *IEEE Transactions on Vehicular Technology*, *59*, 4268–4279. doi:10.1109/TVT.2010.2076320.

Olfati-Saber, R., Fax, J. A., & Murray, R. M. (2007). Consensus and cooperation in networked multi-agent systems. *Proceedings of the IEEE*, *95*, 215–233. doi:10.1109/JPROC.2006.887293.

Petrillo, A., Salvi, A., Santini, S., & Valente, A. S. (2018). Adaptive multi-agents synchronization for collaborative driving of autonomous vehicles with multiple communication delays. *Transportation Research Part C: Emerging Technologies*, *86*, 372–392. doi:10.1016/j.trc.2017.11.009.

Ploeg, J., Shukla, D. P., van de Wouw, N., & Nijmeijer, H. (2014a). Controller synthesis for string stability of vehicle platoons. *IEEE Transactions on Intelligent Transportation Systems*, *15*, 854–865. doi:10.1109/TITS.2013.2291493.

Ploeg, J., van de Wouw, N., & Nijmeijer, H. (2014b). L-p string stability of cascaded systems: Application to vehicle platooning. *IEEE Transactions on Control Systems Technology*, *22*, 786–793. doi:10.1109/TCST.2013.2258346.

Ren, W., & Beard, R. W. (2008). *Distributed consensus in multi-vehicle cooperative control*. Springer.

Ren, W., & Cao, Y. (2010). *Distributed coordination of multi-agent networks: Emergent problems, models, and issues*. Springer Science & Business Media.

Rödönyi, G. (2018). An adaptive spacing policy guaranteeing string stability in multi-brand Ad Hoc platoons. *IEEE Transactions on Intelligent Transportation Systems*, *19*, 1902–1912. doi:10.1109/TITS.2017.2749607.

Seiler, P., Pant, A., & Hedrick, K. (2004). Disturbance propagation in vehicle strings. *IEEE Transactions on Automatic Control*, *49*, 1835–1841. doi:10.1109/TAC.2004.835586.

Shladover, S. E. (2007). PATH at 20 - History and major milestones. *IEEE Transactions on Intelligent Transportation Systems*, *8*, 584–592. doi:10.1109/TITS.2007.903052.

Shladover, S. E., Desoer, C. A., Hedrick, J. K., Tomizuka, M., Walrand, J., Zhang, W.-B., McMahon, D. H., Peng, H., Sheikholeslam, S., & McKeown, N. (1991). Automated vehicle control developments in the PATH program. *IEEE Transactions on Vehicular Technology*, *40*, 114–130. doi:10.1109/25.69979.

Steele, J. M. (2004). *The Cauchy-Schwarz master class: An introduction to the art of mathematical inequalities*. Cambridge University Press.

Stüdli, S., Seron, M. M., & Middleton, R. H. (2017). From vehicular platoons to general networked systems: String stability and related concepts. *Annual Reviews in Control*, *44*, 157–172. doi:10.1016/j.arcontrol.2017.09.016.

Talebpour, A., & Mahmassani, H. S. (2016). Influence of connected and autonomous vehicles on traffic flow stability and throughput. *Transportation Research Part C: Emerging Technologies*, *71*, 143–163. doi:10.1016/j.trc.2016.07.007.

Utkin, V., Guldner, J., & Shi, J. (2009). *Sliding mode control in electro-mechanical systems*. CRC press.

Wang, M. (2018). Infrastructure assisted adaptive driving to stabilise heterogeneous vehicle strings. *Transportation Research Part C: Emerging Technologies*, *91*, 276–295. doi:10.1016/j.trc.2018.04.010.

Xiao, L., & Gao, F. (2011). Practical string stability of platoon of adaptive cruise control vehicles. *IEEE Transactions on Intelligent Transportation Systems*, *12*, 1184–1194. doi:10.1109/TITS.2011.2143407.

Xu, B., Li, S. E., Bian, Y., Li, S., Ban, X. J., Wang, J., & Li, K. (2018). Distributed conflict-free cooperation for multiple connected vehicles at unsignalized intersections. *Transportation Research Part C: Emerging Technologies*, *93*, 322–334. doi:10.1016/j.trc.2018.06.004.

Yadlapalli, S., Darbha, S., & Rajagopal, K. (2006). Information flow and its relation to stability of the motion of vehicles in a rigid formation. *IEEE Transactions on Automatic Control*, *51*, 1315–1319. doi:10.1109/TAC.2006.878723.

Zhang, L., & Orosz, G. (2016). Motif-based design for connected vehicle systems in presence of heterogeneous connectivity structures and time delays. *IEEE Transactions on Intelligent Transportation Systems*, *17*, 1638–1651. doi:10.1109/TITS.2015.2509782.

Zheng, Y., Bian, Y., Li, S., & Li, S. E. (2019). Cooperative control of heterogeneous connected vehicles with directed acyclic interactions. *IEEE Intelligent Tranportation Systems Magazine*, (pp. 1–16). doi:10.1109/MITS.2018.2889654.

Zheng, Y., Li, S. E., Li, K., & Ren, W. (2018). Platooning of connected vehicles with undirected topologies: Robustness analysis and distributed H-infinity controller synthesis. *IEEE Transactions on Intelligent Transportation Systems*, *19*, 1353–1364. doi:10.1109/TITS.2017.2726038.

Zheng, Y., Li, S. E., Wang, J., Cao, D., & Li, K. (2016). Stability and scalability of homogeneous vehicular platoon: Study on the influence of information flow topologies. *IEEE Transactions on Intelligent Transportation Systems*, *17*, 14–26. doi:10.1109/TITS.2015.2402153.

Zhou, J., & Peng, H. (2005). Range policy of adaptive cruise control vehicles for improved flow stability and string stability. *IEEE Transactions on Intelligent Transportation Systems*, *6*, 229–237. doi:10.1109/TITS.2005.848359.

Appendix: Proof of Theorem 2

According to Remark 2, it is required that the platoon should be asymptotically stable, *i.e.*, $k_a \in K_0$, $(k_p, k_v) \in K_1 \cap K_2$. By combining (26a)-(26d) with (16a)-(16c), we have the following four cases:

$$C_0 \geq 0 \Longleftrightarrow k_v \geq \begin{cases} -\frac{h}{2}k_p + \frac{1}{rh}, & l = r, \\ \frac{(r-2)h}{2}k_p + \frac{1}{r^2 h}, & l = 1, \end{cases} \tag{32a}$$

$$C_1 \geq 0 \Longleftrightarrow k_v \leq -hk_p + \frac{2k_a r + 1}{2r\tau}, \tag{32b}$$

$$C_1 < 0 \Longleftrightarrow k_v > -hk_p + \frac{2k_a r + 1}{2r\tau}, \tag{32c}$$

$$\Delta_{\mathrm{d}} \leq 0 \Longleftrightarrow \begin{cases} \tau r\Big(k_v - \dfrac{2k_a r + 1}{2r\tau}\Big)^2 \leq \big((2k_a r + 1)h - 2\tau\big)k_p, & l = r, \\ \tau r\Big(k_v - \dfrac{2k_a r + 1}{2r\tau}\Big)^2 - F_1\Big(k_v - \dfrac{2k_a r + 1}{2r\tau}\Big) + F_0 \leq 0, & l = 1, \end{cases} \tag{32d}$$

where

$$F_1 := 2r(r-1)\tau h k_p,$$
$$F_0 := k_p\left(r(r-1)\tau h\Big((r-1)hk_p - \frac{2k_a r + 1}{r\tau}\Big) + \big(2\tau - (2k_a r + 1)h\big)\right).$$

To sum up, following the sequence of equivalences, we have

$$\text{(22) holds} \Longleftrightarrow \forall l \in \{1, r\},\ \text{(32a)} \wedge \text{(32b) holds, or (32a)} \wedge \text{(32c)} \wedge \text{(32d) holds.} \tag{33}$$

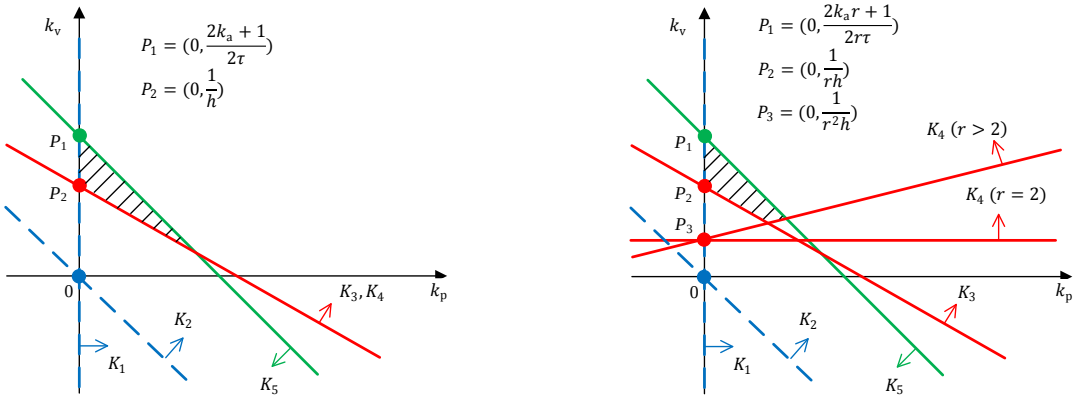

(a) $r = 1$ (b) $r \geq 2$

Figure 7: The feasible region of (k_p, k_v) given by $(K_1 \cap K_2) \cap S_1$

For convenience, denote the feasible region of (k_p, k_v) given in (32a)-(32d) by the following sets:

$$K_3 := \left\{(k_p, k_v) \middle| k_v \geq -\frac{h}{2}k_p + \frac{1}{rh}\right\}, \tag{34a}$$

$$K_4 := \left\{(k_p, k_v) \middle| k_v \geq \frac{(r-2)h}{2}k_p + \frac{1}{r^2 h}\right\}, \tag{34b}$$

$$K_5 := \left\{(k_p, k_v) \middle| k_v \leq -hk_p + \frac{2k_a r+1}{2r\tau}\right\}, \tag{34c}$$

$$K_6 := \left\{(k_p, k_v) \middle| k_v > -hk_p + \frac{2k_a r+1}{2r\tau}\right\}, \tag{34d}$$

$$K_7 := \left\{(k_p, k_v) \middle| r\tau\left(k_v - \frac{2k_a r+1}{2r\tau}\right)^2 \leq \left((2k_a r+1)h - 2\tau\right)k_p\right\}, \tag{34e}$$

$$K_8 := \left\{(k_p, k_v) \middle| r\tau\left(k_v - \frac{2k_a r+1}{2r\tau}\right)^2 - F_1\left(k_v - \frac{2k_a r+1}{2r\tau}\right) + F_0 \leq 0\right\}. \tag{34f}$$

Necessity. Assume that there exists a set of feedback gains $k = [k_p, k_v, k_a]^\top$ such that (22) holds. According to (33), either (32a) $\wedge$ (32b) or (32a) $\wedge$ (32c) $\wedge$ (32d) holds when $l = r$. On the one hand, if (32a) $\wedge$ (32b) holds, combining (32a), (32b), and $l = r$ yields

$$-\frac{h}{2}k_p + \frac{1}{rh} \leq k_v \leq -hk_p + \frac{2k_a r+1}{2r\tau},$$

which implies (29). On the other hand, if (32a) $\wedge$ (32c) $\wedge$ (32d) holds, since $(k_p, k_v) \in K_1 \cap K_2 \Longrightarrow k_p > 0$, combining (32d) and $l = r$ yields

$$(2k_a r+1)h - 2\tau \geq 0,$$

which also implies (29).

Sufficiency. Assume that (29) holds.

When $h > \frac{2\tau}{2k_a r+1}, k_a > -\frac{1}{2r}$, we consider the following two sets:

$$S_1 := K_3 \cap K_4 \cap K_5,$$
$$S_2 := K_3 \cap K_4 \cap K_6 \cap K_7 \cap K_8.$$

Given a set of parameters h, k_a, r, and τ, the feasible regions of (k_p, k_v) given by $(K_1 \cap K_2) \cap S_1$ and $(K_1 \cap K_2) \cap S_2$ are shown in Figure 7 and Figure 8, respectively. Here, we use the fact that the outlines of K_7 and K_8 are both quadratic parabola curves. In these figures, dash lines indicate open sets while solid lines indicate closed sets. In addition, forward slashes indicate the feasible regions. It is easy to check that $(K_1 \cap K_2) \cap S_1$ and $(K_1 \cap K_2) \cap S_2$ are not empty. Moreover, $(k_p, k_v) \in S_1$ implies that (32a) $\wedge$ (32b) holds, and $(k_p, k_v) \in S_2$ implies that (32a) $\wedge$ (32c) $\wedge$ (32d) holds. Then, according to (33), we know that $\forall (k_p, k_v) \in (K_1 \cap K_2) \cap (S_1 \cup S_2)$, (22) holds.

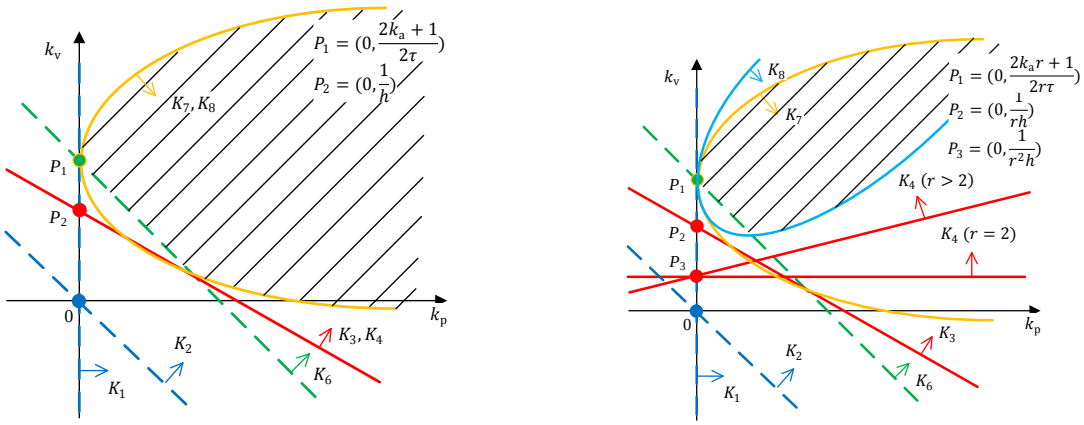

(a) $r = 1$ (b) $r \geq 2$

Figure 8: The feasible region of (k_p, k_v) given by $(K_1 \cap K_2) \cap S_2$

When $h = \frac{2\tau}{2k_a r+1}, k_a > -\frac{1}{2r}$, we define the following feasible region of (k_p, k_v):

$$K_9 := \left\{(k_p, k_v) \middle| k_p(r-2) \leq \frac{r-1}{r}\frac{(2k_a r+1)^2}{2r\tau^2}, k_v = \frac{2k_a r+1}{2r\tau}\right\},$$
$$K_{10} := \left\{(k_p, k_v) \middle| k_p(r-1) \leq \frac{(2k_a r+1)^2}{2r\tau^2}, k_v = \frac{2k_a r+1}{2r\tau}\right\},$$

and we consider the following set

$$S_3 = K_9 \cap K_{10}.$$

It is not difficult to check that $(K_1 \cap K_2) \cap S_3$ is not empty. Then $\forall (k_p, k_v) \in (K_1 \cap K_2) \cap S_3$, we have:

$$k_v + \frac{h}{2}k_p - \frac{1}{rh} = \frac{h}{2}k_p > 0, \tag{35a}$$
$$k_v - \frac{(r-2)h}{2}k_p - \frac{1}{r^2 h} = \frac{2k_a r+1}{2r\tau}\frac{r-1}{r} - \frac{(r-2)h}{2}k_p \geq 0, \tag{35b}$$
$$k_v + hk_p - \frac{2k_a+1}{2r\tau} = \frac{2\tau}{2k_a r+1}k_p > 0, \tag{35c}$$
$$r\tau\left(k_v - \frac{2k_a r+1}{2r\tau}\right)^2 - \big((2k_a r+1)h - 2\tau\big)k_p = 0, \tag{35d}$$
$$r\tau\left(k_v - \frac{2k_a r+1}{2r\tau}\right)^2 - F_1\left(k_v - \frac{2k_a r+1}{2r\tau}\right) + F_0 = r(r-l)\tau h k_p\big(hk_p(r-l) - 2k_v\big) \leq 0. \tag{35e}$$

Since (35a) $\wedge$ (35b) $\Longrightarrow (k_p, k_v) \in K_3 \cap K_4$, (35c) $\Longrightarrow (k_p, k_v) \in K_6$, (35d) $\wedge$ (35e) $\Longrightarrow (k_p, k_v) \in K_7 \cap K_8$, we have $(k_p, k_v) \in K_3 \cap K_4 \cap K_6 \cap K_7 \cap K_8 = S_2$, which implies that (32a) $\wedge$ (32c) $\wedge$ (32d) holds. Then according to (33), $\forall (k_p, k_v) \in (K_1 \cap K_2) \cap S_3$, (22) holds.

To sum up, there exists a set of feedback gains $k = [k_p, k_v, k_a]^\top$ such that (22) holds.

□